Pharmaceutica Analytica Acta
ISSN: 2153-2435

Dar et al., Pharm Anal Acta 2016, 7:2
DOI: 10.4172/2153-2435.1000464

Research Article Open Access

DNA Binding, Cleavage Activity, Molecular Docking, Cytotoxicity and Genotoxicity Studies of Newly Synthesized Copper Based Metal Complexes

Ayaz Mahmood Dar[1,2]*, Meraj Alam Khan[1], Shafia Mir[2] and Manzoor Ahmad Gatoo[3]

[1]Department of Chemistry, Aligarh Muslim University, Aligarh 202002, India
[2]Department of Chemistry, Government Degree College, Kulgam 192231, J&K, India
[3]Department of Biochemistry JNMC, Aligarh Muslim University, Aligarh 202002, India

Abstract

The design and synthesis of medicinal chemotherapeutic agents of copper with 2-(benzothiazol-2-yl iminomethyl)-phenol, 2-(benzothiazol-2-yliminomethyl)-valine, cyanoaceto (2-mer- captobenzylidene)-hydrazide, 2-(phenacyl bromide)-aminothiophenol, (2-mercaptobenzaldehyde) thio- semicarbazone, N-(phenacyl bromide)-2-yliminobenzothiazole, 2-aminobenzothiazole, benzothiazol-2-yliminomethyl)-phenol and 2-[(2'-aminobenzylidene)-amino]-benzenethiol were synthesized. The characterization was done by FTIR, 1H and 13C NMR, MS, TGA and elemental analysis. Interaction of complexes 8 and 9 with CT DNA was done by using UV-vis and fluorescence spectroscopy depicting the hyperchromic behaviour of complexes. The intrinsic binding constants (Kb) for complex 8 and 9 were 2.35×10^3 M^{-1} and 2.12×10^3 M^{-1}. The cleavage studies of complex 8 and 9 were done with pBR322 plasmid showing the potential cleaving ability of the complexes at very low concentration. The gel electrophoresis pattern also demonstrated that the complex 8 alone or in presence of Cu (II) causes the nicking of supercoiled pBR322 and it seems to follow the mechanistic pathway involving generation of hydroxyl radicals that are responsible for initiating DNA strand scission. The molecular docking studies showed the minor groove binding behaviour of the complexes 8 and 9 with DNA. During the MTT assay against different cancer cell lines like SW480, HepG2, HT29 and HL60, all the complexes showed potential cytotoxic behaviour by giving effective IC50 close to Cisplatin. The bioactivity score and PASS analysis also depicted the drug like nature of the complexes. During the comet assay, apoptotic degradation of DNA in the presence of complex 8 and 9 was analysed by agarose gel electrophoresis and visualized by ethidium bromide staining.

Keywords: Copper complexes; UV-vis and fluorescence; DNA; MTT; Comet; Docking

Introduction

The pharmacology of heterocyclic ligands and their metal chelates is focus of research for bioinorganic chemists [1]. The nitrogen containing organic compounds and their metal complexes display a wide range of biological activities [2-4] e.g. antitumor, antibacterial, antifungal and antiviral properties. Metal complexes that can bind to DNA are gaining considerable attention due to their diverse applications as new generation metallo-pharmaceuticals [5].

The production of new therapeutic modulaties for cancer chemotherapy is the subject of immense interest owing to the fact that many present treatment regimes (platinum-based drugs) in chemotherapy have failed or fall short either in terms of efficiency or toxicity problems associated with them [6,7]. Among the non-platinum complexes for metal based chemotherapy, copper complexes have been much explored due to the fact that copper is bio-essential element responsible for numerous bioactivities in living organism [8]. Copper being redox active exists in biologically accessible +2/+1 oxidation states and is an important co-factor of several enzymes involved in oxidative metabolism, ceruloplasmine, superoxide dismutase, ascorbic acid oxidase and tyrosinase [9].

In addition to this, in recent years there has been a rapid expansion in the development of metal complexes as extensive diagnostic agents [6]. In this regard therapeutic agents that pertain to less toxic and more effective metallic component like Cu(II) are of particular interest and include a plethora of compounds: antitumor, antioxidant, antimicrobial and antiflammatory agents [10]. The appropriate redox property of Cu(II) is essential for various metabolic pathways like mitochondrial respiration, free radical scavenging, and iron absorption where it acts as a catalytic cofactor [11]. The Cu(II) complexes follows different mode of action towards DNA (non-covalent) as compared to cisplatin (covalent). Therefore, Cu(II)-based generic complexes exhibit higher antineoplastic potency towards human ovarian carcinoma, leukaemia, and various cervicouterine carcinomas as compared to cisplatin [12]. A large number of chemotherapeutic agents imply potentially useful therapeutic strategies and elicit antitumor effect by inducing cancer cell apoptosis by generating large amount of noxious radicals into the cancer cells [13]. Keeping in view the applications of coordination complexes, we here in report the synthesis, DNA binding studies, cleavage activity, molecular docking studies and *in vitro* cytotoxicity of Bis [2-(benzothiazol-2-yl iminomethyl)-phenol] copper 1, Bis [2-(benzothiazol-2-yliminomethyl)-valine] copper 2, Bis [cyanoaceto (2-mercaptobenzylidene)-hydrazide] copper 3, Bis [2-(phenacyl bromide)-aminothiophenol] copper 4, Bis [(2-mercaptobenzaldehyde) thiosemicarbazone] copper 5, Bis [N-(phenacyl bromide)-2-

***Corresponding author:** Ayaz Mahmood Dar, Department of Chemistry Aligarh Muslim University Aligarh 202002 India, Tel: +91-9286990247; E-mail: ayazchem09@gmail.com

Received January 27, 2016; **Accepted** February 05, 2016; **Published** February 08, 2016

Citation: Dar AM, Khan MA, Mir S, Gatoo MA (2016) DNA Binding, Cleavage Activity, Molecular Docking, Cytotoxicity and Genotoxicity Studies of Newly Synthesized Copper Based Metal Complexes. Pharm Anal Acta 7: 464. doi:10.4172/2153-2435.1000464

yliminobenzothiazole] copper 6, Bis (2-aminobenzothiazole) copper 7, Bis [2-(benzothiazol-2-yliminomethyl)-phenol] copper 8 and Bis 2-[(2′-aminobenzylidene)-amino]-benzenethiol copper 9 complexes.

Experimental

Materials and methods

All chemicals were purchased from Sigma-Aldrich (India) and Merck (India). Melting points were determined on a Kofler apparatus and are uncorrected. The IR spectra were recorded on KBr pellets with Perkin Elmer RXI Spectrometer and values are given in cm^{-1}. 1 H and 13 C NMR spectra were run in $CDCl_3$ on a JEOL Eclipse (400 MHz) instrument with TMS as internal standard and values are given in ppm (δ). Mass spectra were recorded on a JEOL SX102/DA-6000 Mass Spectrometer. Carbon, hydrogen and nitrogen contents were determined on Carlo Erba Analyzer Model 1106. Calcium chloride (anhydrous) was used as a drying agent. Electronic spectra were recorded on UV-1700 PharmaSpec UV-Vis spectrophotometer (Shimadzu). Fluorescence measurements were made on SCHIMADZU RF-5301 fluorescence spectrophotometer. Super coiled pBR322 DNA was purchased from GeNei (India) and was used for the agarose gel experiment without further purification. Double-stranded calf thymus DNA, purchased from Sigma, was dissolved in a 0.1 M Tris-buffer. The purity of DNA was verified by monitoring the ratio of absorbance at 260 nm to that of 280 nm, which was in the range 1.8-1.9. The concentration of the DNA was determined spectrophotometrically using ε260 = 6600 M^{-1} cm^{-1}. The human cancer cell lines used for the cytotoxicity experiment were SW480, HepG2, HT-29 and HL-60 which were obtained from National Cancer Institute (NCI), biological testing branch, Federick Research and Development Centre, USA. The treated and control cancer cells were viewed with a FluoView FV1000 (Olympus, Tokyo, Japan) confocal laser scanning microscope (CLSM) equipped with argon and HeNe lasers.

Procedure for the synthesis of new copper complexes (1-9)

Bis [2-(benzothiazol-2-yliminomethyl)-phenol] copper (1): It was prepared by a general synthetic method in which methanolic solution (20 ml) of $CuSO_4.5H_2O$ (0.233 g, 1 mmol) was added to the methanolic solution of 2-aminobenzothiazole (0.150 g, 1 mmol) and 2-hydroxybenzaldehyde (0.122 g, 1 mmol) in a 1:1:1 molar ratio which was refluxed for 1.5 h to obtain a greenish colour solution. The coloured product was isolated, washed with water and dried in vacuo to get pure powder.

Yield 82%. M.p. 241°C. Anal. Calc (%) for $C_{28}H_{20}CuN_4O_2S_2$: C, 58.78; H, 3.52; N, 9.79. Found: C, 58.62; H, 3.35; N, 9.49; IR (KBr, ν cm^{-1}) 3335 (OH), 1649 (HC=N), 1630-1619 (aromatic), 1440 (C-N), 430 (Cu-N), 422 (Cu-S); ^{1}H NMR ($CDCl_3$, 400 MHz): δ 8.31, 7.92 (s, 1H, 2 × OH exchangeable with D_2O), 6.35-7.41 (m, 8H, 2 × 8 aromatic ring protons), 7.16, (s, 1H, 2 × HC=N); ^{13}C NMR ($CDCl_3$, 100 MHz): δ 112-133 (2 × 12 aromatic carbon signals), 151, 149 (2 × HC=N); ESI-MS (m/z): 572 $[C_{28}H_{20}CuN_4O_2S_2]^+$.

Bis [2-(benzothiazol-2-yliminomethyl)-valine] copper (2): It was synthesized by a general synthetic method in which methanolic solution (20 ml) of $CuSO_4.5H_2O$ (0.233 g, 1 mmol) was added to the methanolic solution of 2-aminobenzothiazole (0.150 g, 1 mmol) and L-valine (0.177 g, 1 mmol) in a 1:1:1 molar ratio which was refluxed for 2 h to obtain a bluish green solution. The coloured product was isolated, washed with water and dried in vacuo to get pure powder.

Yield 75%. M.p. 232°C. Anal. Calc (%) for $C_{24}H_{30}CuN_6O_2S_2$: C, 51.27; H, 5.38; N, 14.95; S, 11.41. Found: C, 51.13; H, 5.19; N, 14.81; S, 11.29. IR (KBr, ν cm^{-1}) 3342 (OH), 3256 (NH_2) 1636-1616 (aromatic), 1657 (C=N), 1440 (C-N), 427 (Cu-N), 410 (Cu-S); ^{1}H NMR ($CDCl_3$, 400 MHz): δ 8.11, 8.24 (s, 1H, 2 × OH exchangeable with D_2O), 6.63-6.93 (m, 8H, 2 × 4 aromatic ring protons), 4.34 (br s, 2H, 2 × NH_2 exchangeable with D_2O), 2.44, 2.39 (d, 1H, 2 × CH-$(CH_3)_2$), 2.15, 2.11 (m, 1H, 2 × $(CH_3)_2$-CH, 1.3 (d, 6H, $(CH_3)_2$-CH); ^{13}C NMR ($CDCl_3$, 100 MHz): δ 122-153 (2 × 6 aromatic carbon signals), 162.4-165 (4 × C=N), 62, 60.6 (C-N); ESI-MS (m/z): 561 $[C_{24}H_{30}CuN_6O_2S_2]^+$.

Bis [cyanoaceto (2-mercaptobenzylidene)-hydrazide] copper (3): It was prepared by a general synthetic method in which methanolic solution (15 ml) of $CuSO_4.5H_2O$ (0.233 g, 1 mmol) was added to the methanolic solution of 2-merceptobenzaldehyde (0.138 g, 1 mmol) and cyanoacetohydrazide (0.099 g, 1 mmol) in a 1:1:1 molar ratio which was refluxed for 1.5 h to obtain a reddish solution. The coloured product was isolated, washed with water and dried in vacuo to get pure powder.

Yield 78%. M.p. 237°C. Anal. Calc (%) for $C_{20}H_{16}CuN_6O_2S_2$: C, 48.04; H, 3.23; N, 16.81; S, 12.82. Found: C, 47.89; H, 3.16; N, 16.64; S, 12.57. IR (KBr, ν cm^{-1}) 3215 (NH), 1678 (CO NH), 2242 (C≡N), 1654 (C=N), 1627-1618 (aromatic), 1436 (C-N), 435 (Cu-N), 412 (Cu-S); ^{1}H NMR ($CDCl_3$, 400 MHz): δ 8.3, 8.1 (s, 1H, 2 × NH exchangeable with D_2O), 7.72 (s, 1 H, 2 × HC=N), 6.53-7.16 (m, 8 H, 2 × 4 aromatic ring protons), 3.75 (s, 2H, 2 × CH_2); ^{13}C NMR ($CDCl_3$, 100 MHz): δ 171, 171.3 (2 × C=O), 157, 155 (2 × C=N), 125-133 (2 × 6 aromatic carbon signals), 119, 121 (2 × C≡N); ESI-MS (m/z): 499 $[C_{20}H_{16}CuN_6O_2S_2]^+$.

Bis [2-(phenacyl bromide)-aminothiophenol] copper (4): It was also synthesized by a general synthetic method in which methanolic solution of 2-aminothiophenol (0.125 g, 1 mmol), phenacyl bromide (0.199 g, 1 mmol) and (20 ml) of $CuSO_4.5H_2O$ (0.233 g, 1 mmol) were added to the in a 1:1:1 molar ratio and was refluxed for 1.5 h to obtain a yellow solution. The coloured product was isolated, washed with water and dried in vacuo to get pure powder.

Yield 75%. M.p. 224°C. Anal. Calc (%) for $C_{28}H_{24}CuN_2O_2S_2$: C, 61.35; H, 4.41; N, 5.11; S, 11.70. Found: C, 61.19; H, 4.28; N, 5.04; S, 11.52. IR (KBr, ν cm^{-1}) 3213 (NH), 1675 (CO), 1625-1638 (aromatic), 1436 (C-N), 435 (Cu-N), 412 (Cu-S); ^{1}H NMR ($CDCl_3$, 400 MHz): δ 6.27-6.61 (m, 8H, 2 × 4 protons of aminothiophenol moiety), 6.83-7.12 (m, 12H, 2 × 5 protons of phenacyl moiety), 4.3, 4.2 (s, 1H, 2 × NH exchangeable with D_2O), 4.72 (s, 1H, 2 × H_2C-CO), 3.75 (s, 2H, 2 × CH_2); ^{13}C NMR ($CDCl_3$, 100 MHz): δ 168, 170 (2 × C=O), 129-145 (2 × 6 aromatic carbon signals of phenacyl moiety), 116-132 (2 × 6 aromatic carbon signals of aminothiophenol moiety); 62, 65 (2 × CH_2); ESI-MS (m/z): 548 $[C_{28}H_{24}CuN_2O_2S_2]^+$.

Bis [(2-mercaptobenzaldehyde) thiosemicarbazone] copper (5): It was prepared by a general synthetic method in which methanolic solution (20 ml) of $CuSO_4.5H_2O$ (0.233 g, 1 mmol) was added to the methanolic solution of 2-merceptobenzaldehyde (0.138 g, 1 mmol) and thiosemicarbazide (0.091 g, 1 mmol) in a 1:1:1 molar ratio which was refluxed for 1 h to obtain an off white solution. The coloured product was isolated, washed with water and dried in vacuum to get pure powder.

Yield 76%. M.p. 247°C. Anal. Calc (%) for $C_{16}H_{16}CuN_6S_4$: C, 39.69; H, 3.33; N, 17.36; S, 26.49. Found: C, 39.56; H, 3.21; N, 17.14; S, 26.35. IR (KBr, ν cm^{-1}) 3230, 3177 (NH, NH_2), 1654 (C=N), 1619-1631 (aromatic), 1436 (C-N), 435 (Cu-N), 414 (Cu-S), 537 (C=S); ^{1}H NMR ($CDCl_3$, 400 MHz): δ 7.7, 7.4 (s, 1H, 2 × HC=N), 7.1-7.51 (m, 8H, 2 × 4 aromatic protons), 3.6 (s, 1H, 2 × NH exchangeable with D_2O), 3.7 (s, 1H, 2 × NH_2 exchangeable with D_2O); ^{13}C NMR ($CDCl_3$, 100 MHz): δ 181, 178 (2 × C=S), 154, 151 (2 × C=N), 125-134 (2 × 6 aromatic carbon signals); ESI-MS (m/z): 484 $[C_{16}H_{16}CuN_6S_4]^{+\cdot}$

Bis [N-(phenacyl bromide)-2-yliminobenzothiazole] copper (6): It was prepared by a general synthetic method in which methanolic solution (20 ml) of $CuSO_4.5H_2O$ (0.233 g, 1 mmol) was added to the methanolic solution of 2-aminobenzothiazole (0.150 g, 1 mmol) and phenacyl bromide (0.199 g, 1 mmol) in a 1:1:1 molar ratio which was refluxed for 2 h to obtain a dark green solution. The coloured product was isolated, washed with water and dried in vacuo to get pure powder.

Yield 80%. M.p. 253°C. Anal. Calc (%) for $C_{30}H_{26}CuN_4O_2S_2$: C, 59.83; H, 4.35; N, 9.30; S, 10.65. Found: C, 59.69; H, 4.20; N, 9.16; S, 10.43. IR (KBr, ν cm^{-1}) 3224 (NH), 1693 (C=O), 1651 (C=N), 1621-1634 (aromatic), 1436 (C-N), 435 (Cu-N), 417 (Cu-S); ^{1}H NMR ($CDCl_3$, 400 MHz): δ 6.27-6.61 (m, 8H, 2 × 4 protons of 2-aminothiazole moiety), 6.83-7.12 (m, 10H, 2 × 5 protons of phenacyl moiety), 4.3 (s, 1H, 2 × NH exchangeable with D_2O), 4.72 (s, 1H, 2 × H_2C-CO); ^{13}C NMR ($CDCl_3$, 100 MHz): δ 164, 167 (2 × C=O), 147, 144 (2 × C=N), 129-145 (2 × 6 aromatic carbon signals of phenacyl moiety), 121-128 (2 × 6 aromatic carbon signals of 2-aminothiazole moiety); 61, 63 (2 × CH_2); ESI-MS (m/z): 602 $[C_{30}H_{26}CuN_4O_2S_2]^+$.

Bis (2-aminobenzothiazole) copper (7): It was also synthesized by a general synthetic method in which methanolic solution (20 ml) of $CuSO_4.5H_2O$ (0.233 g, 1 mmol) was added to the methanolic solution of 2-aminobenzothiazole (0.150 g, 1 mmol) in a 1:1 molar ratio which was refluxed for 55 min. to obtain a leaflet green solution. The coloured product was isolated, washed with water and dried in vacuum to get pure powder.

Yield 81%. M.p. 264°C. Anal. Calc (%) for $C_{14}H_{12}N_4O_{10}S_2Cu$: C, 46.20; H, 3.32; N, 15.39; S, 17.62. Found: C, 46.12; H, 3.23; N, 15.33; S, 17.59. IR (KBr, ν cm^{-1}) 3221 (NH_2), 1624-1617 (aromatic), 1641 (C=N), 1429 (C-N), 428 (Cu-N), 645 (C-S). ^{1}H NMR ($CDCl_3$, 400 MHz): δ 8.2-7.1 (m, 8 H, 2 × aromatic ring 4 protons), 3.72 (s, 4 H, 2 × NH_2 exchangeable with D_2O). ^{13}C NMR ($CDCl_3$, 100 MHz): δ 122-156 (2 × 6 aromatic carbon signals), 145 (C=N), 134 (C-N), 120 (C-S). ESI-MS (m/z): 362 $[C_{14}H_{12}N_4O_{10}S_2Cu]^+$.

Bis [2-(Benzothiazol-2-yliminomethyl)-phenol] copper (8): It was prepared by adding salicyaldehyde (0.122 g, 1 mmol), 2-aminobenzothiazole (0.150 g, 1mmol) to a methanolic solution (20 ml) of $CuSO_4.5H_2O$ (0.233 g, 1 mmol) in a 1:1:1 molar ratio. The reaction mixture was refluxed for 50 min. at room temperature. The greenish-yellow precipitate which formed was filtered off under vacuum, washed thoroughly with water and dried in vacuo over anhydrous $CaCl_2$.

Yield: 76%. M.p. 279°C. Anal. Calc (%) for $C_{28}H_{18}CuN_4O_2S_2$: C, 58.99; H, 3.18; N, 9.83; S, 11.25. Found: C, 58.92; H, 3.13; N, 9.78; S, 11.21. IR (KBr, ν cm^{-1}) 1621-1615 (aromatic), 1647 (C=N), 1633 (HC=N), 1440 (C-N), 1082 (C-O), 448 (Cu-O), 647 (C-S). ^{1}H NMR ($CDCl_3$, 400 MHz): δ 8.2-7.1 (m, 16H, 2× aromatic ring 8 protons), δ 8.14 (s, 1H, HC=N), δ 8.11 (s, 1H, HC=N). ^{13}C NMR ($CDCl_3$, 100 MHz): δ 121-158 (2×12 aromatic carbon signals), 158, 149 (C=N). ESI-MS (m/z): 570 $[C_{28}H_{18}N_4O_2S_2Cu]^+$.

Bis 2-[(2′-Amino-benzylidene)-amino]-benzenethiol copper (9): It was prepared by adding 2-aminobenzaldehyde (0.121 g, 1 mmol), 2-aminothiophenol (0.125 g, 1mmol) to a methanolic solution (20 ml) of $CuSO_4.5H_2O$ (0.233 g, 1 mmol) in a 1:1:1 molar ratio. The reaction mixture was refluxed for 50 min. at room temperature. The reddish precipitate which formed was filtered off under vacuum, washed thoroughly with water and dried in vacuo over anhydrous $CaCl_2$.

Yield: 79%. M.p. 284°C. Anal. Calc (%) for $C_{26}H_{22}N_4S_2Cu$: C, 60.27; H, 4.28; N, 10.81; S, 12.38. Found: C, 60.23; H, 4.19; N, 10.77; S, 12.35. IR (KBr, ν cm^{-1}) 1628-1619 (aromatic), 1643 (HC=N), 1434 (C-N), 424 (Cu-N), 651 (C-S). ^{1}H NMR ($CDCl_3$, 400 MHz): δ 8.1-7.04 (m, 16H, 2 × aromatic ring 8 protons), δ 8.39 (s, 1 H, HC=N), δ 8.27 (s, 1 H, HC=N), δ 4.14 (s, 1 H, NH_2 exchangeable with D_2O), δ 3.92 (s, 1 H, NH_2 exchangeable with D_2O). ^{13}C NMR ($CDCl_3$, 100 MHz): δ 117-157 (2 × 12 aromatic carbon signals), 163, 161 (C=N). ESI-MS (m/z): 518 $[C_{26}H_{22}N_4S_2Cu]^+$.

DNA binding studies

Cleavage experiments were performed with Axygen agarose electrophoresis [14] connected to a Genei 50-500 V power supply visualized and photographed by the Vilber-INFINITY gel documentation system. Cleavage experiments of supercoiled pBR322 DNA (300 ng) by complex 8 and 9 (1.0-7.0 μM) in a 5 mM Tris-HCl / 50 mM NaCl buffer at pH 7.2 were carried out and the reaction followed by Agarose gel electrophoresis. The samples were incubated for 1 h at 37°C. A loading buffer, containing 25% bromophenol blue, 0.25% xylene cyanol and 30% glycerol, was added and electrophoresis was carried out at 60 V for 1 h in a Tris-HCl buffer using a 1% agarose gel containing 1.0 mg/mL of ethidium bromide.

Absorption and emission spectroscopy was used to investigate further the binding affinity of complexes. It involves the standard methods and practices reported in the literature [15-17]. While measuring the absorption spectra, an equal amount of DNA was added to both the complex solution and the reference solution to eliminate the absorbance of the DNA itself, Tris buffer was subtracted through base line correction.

Anticancer activity

Cell lines and culture conditions: Human cancer cell lines SW480 (colon adenocarcinoma), HepG2 (hepatic carcinoma), HT-29 (Colon carcinoma) and HL-60 (human leukaemia) were taken for the study. The cells were grown in RPMI 1640 supplemented with 10% fetal bovine serum (FBS), 10U penicillin and 100 μg/mL streptomycin at 37°C with 5% CO_2 in a humidified atmosphere. Fresh medium was given every second day and on the day before the experiments were done. Cells were passaged at pre-confluent densities, using a solution containing 0.05% trypsin and 0.5 mM EDTA.

Cell viability assay (MTT): The anticancer activity *in vitro* was measured using the MTT assay [18,19]. Exponentially growing cells were harvested and plated in 96-well plates at a concentration of 1 × 10^4 cells/well. After 24 h incubation at 37°C under a humidified 5% CO_2 to allow cell attachment, the cells in the wells were respectively treated with target complexes at various concentrations for 48 h. The concentration of DMSO was always kept below 1.25%, which was found to be non-toxic to the cells. A solution of 3-(4,5-dimethylthizao1-2-y1)-2,5-diphenyltetrazolium bromide (MTT), was prepared at 5 mg/mL in phosphate buffered saline (PBS; 1.5 mM KH_2PO_4, 6.5 mM Na_2HPO_4, 137 mM NaCl, 2.7 mM KCl; pH 7.4). 20 μL of this solution were added to each well. After incubation for 4 h at 37°C in a humidified incubator with 5% CO_2, the medium/MTT mixtures were removed and the formazan crystals formed by the mitochondrial dehydrogenase activity of vital cells were dissolved in 100 μL of DMSO per well. The absorbance of the wells was read with a microplate reader (Bio-Rad Instruments) at 570 nm. Effects of the drug cell viability were calculated using cells treated with DMSO as control. Cancer cells were grown on glass cover slips in 12-well cell culture plates (CoStar). After incubation with the test complexes, the disks were flipped on glass plates and the treated and control cancer cells were observed with a FluoView FV1000

(Olympus, Tokyo, Japan) confocal laser scanning microscope (CLSM) equipped with argon and HeNe lasers.

Data analysis: Cell survival was calculated using the formula: Survival (%) = [(absorbance of treated cells-absorbance of culture medium) / (absorbance of untreated cells - absorbance of culture medium)] × 100 [20]. The experiment was done in triplicate and the inhibitory concentration (IC) values were calculated from a dose response curve. IC_{50} is the concentration in 'μM' required for 50% inhibition of cell growth as compared to that of control. IC_{50} values were determined from the linear portion of the curve by calculating the concentration of agent that reduced absorbance in treated cells, compared to control cells, by 50%. Evaluation is based on mean values from three independent experiments, each comprising at least six microcultures per concentration level.

Comet assay (Single cell gel electrophoresis)

The comet assay [21] was performed to evaluate the genotoxic effect of the copper complexes 8 and 9 in HT-29 cells. HT-29 (1×10^6) cells were treated with three different concentrations, 10, 25 and 50 mg/mL of copper complexes 8 and 9 in for 24 h. The cells were then washed and 200 mL of cell suspension in low melting agarose (LMA) were layered onto the labelled slides precoated with agarose (1.5%). The slides were placed on ice for 10 min and submerged in a lysis buffer (2.5% NaCl, 100 mM EDTA, 10 mM Tris, 10% DMSO and 1% Troton X-100) at 48°C at pH 10 for more than 1 h. The slides were then equilibrated in an alkaline buffer (30 mM NaOH, 1 mM EDTA) at pH 13 at 48°C, electrophoresed at 0.86 V/cm at 48°C, neutralized, washed, and dried. At the time of capturing the images, the slides were stained with ethidium bromide (EtBr, 150 mL 1X) and cover slips were placed over them. For visualization of DNA damage, EtBr-stained slides were observed under 209 objectives of a fluorescent microscope (Olympus BX-51, Japan). The images of 50-100 randomly selected cells were captured per slide using a CCD camera.

Molecular docking

The rigid molecular docking studies were performed using HEX 6.1 software [22]. The initial structure of the copper complexes 8 and 9 was generated by Discovery studio software. The molecules of complexes 8 and 9 were optimized for use in the following docking study. The crystal structure of the B-DNA dodecamer d(CGCAAATTTCGC)2 (PDB ID: 1BNA) were downloaded from the protein data bank. All calculations were carried out on an Intel CORE i5, 2.6 GHz based machine running MS Windows 7 as the operating system. Visualization of the docked pose have been done using PyMol molecular graphics program [23].

Determination of physicochemical properties: Bioactivity score and PASS (Prediction of biological activity spectra) analysis: The physicochemical parameters including octanol partition coefficients (miLogP), HBD, HBA, TPSA and Rotatable bonds were calculated using molinspiration server (http://www.molinspiration.com/cgi-bin/properties) and ChemAxon (chemicalize.org). The PASS (Prediction of biological activity spectra) approach is based on the structure-activity correlation, Complex activity prediction is done by "comparing" the structure of query compound with the structure of well-known biological active substrate existing in database of the freely available PASS web service. Complex activity prediction is done by "comparing" the structure of query complex with the structure of well-known biological active substrate existing in database of PASS web service.

Result and Discussion

Chemistry

Development of highly functional coordination complexes from simple building blocks has always been the curiosity of synthetic inorganic chemists. So we here in report the convenient synthesis of Bis [2-(benzothiazol-2-yl iminomethyl)-phenol] copper 1, Bis [2-(benzothiazol-2-yliminomethyl)-valine] copper 2, Bis [cyanoaceto (2-mercaptobenzylidene)-hydrazide] copper 3, Bis [2-(phenacyl bromide)-aminothiophenol] copper 4, Bis [(2-mercaptobenzaldehyde) thiosemicarbazone] copper 5, Bis [N-(phenacyl bromide)-2-yliminobenzothiazole] copper 6, Bis (2-aminobenzothiazole) copper 7, Bis [2-(benzothiazol-2-yliminomethyl)-phenol] copper 8 and Bis 2-[(2′-aminobenzylidene)-amino]-benzenethiol copper 9 by reacting 2-(benzothiazol-2-yl iminomethyl)-phenol, 2-(benzothiazol-2-ylimino methyl)-valine, cyanoaceto (2-mercaptobenzylidene)-hydrazide, 2-(phenacyl bromide)-aminothio- phenol, (2-mercaptobenzaldehyde) thiosemicarbazone, N-(phenacyl bromide)-2-yliminobenzo- thiazole, 2-aminobenzothiazole, benzothiazol-2-yliminomethyl)-phenol and 2-[(2′-amino benzylidene)-amino]-benzenethiol with copper sulphate, respectively in 1:1 ratio in methanol for the period of about 1-2.5 h under reflux conditions (Scheme 1) and on the completion of reaction, new complexes 1-9 were obtained in potential yield of 75-82%.

All the new complexes were stable towards air and moisture and soluble in DMSO. The complexes were thoroughly characterized from spectroscopic (IR, ^{1}H NMR, ^{13}C NMR, TGA and MS) and analytical data (Experimental section). The spectral data is in good agreement with the proposed structures of copper heterocyclic complexes. In the IR spectra, the absorption bands in the range 3177-3256 cm^{-1} show the presence of NH_2 in the compounds while as the absorption bands at 3335-3342, 1633-1657, 3213-3230, 1675-1693, 424-435 and 410-422 cm^{-1} confirm the presence of OH, C=N, NH, C=O, Cu-N and Cu-S, respectively in complexes (1-9). In ^{1}H NMR study, the absorption at δ 8.31-7.92 confirmed the presence of OH while as the absorption peaks at δ 4.34-3.6 revealed the presence of NH_2 in complexes (1-9). The presence of signals (multiplet) at δ 6.35-7.41 depicted the aromatic moiety in complexes (1-9) while as absorption at δ 4.3-4.2 and δ 8.3-8.1 showed the presence of NH attached to groups primary and secondary carbon atoms in complexes (1-9). In ^{13}C NMR study, the signals at δ 144-165, δ 1164-173, δ 181-178 revealed the presence of C=N, C=O and C=S while as signals in the range of δ 112-145 confirm the presence of aromatic ring carbons in complexes (1-9). Finally the presence of distinct molecular ion peak [$M^{+\cdot}$] at m/z: 572, 561, 499, 548, 484, 602, 362, 570 and 518 in the MS also proved the formation of complexes 1-9, respectively.

Thermo gravimetric analysis (TGA)

To examine the thermal stability of complexes 1 and 2, the thermogravimetric analysis were carried out under nitrogen atmosphere in the temperature range 700°C at a heating rate of 20°C min^{-1} (Figure 1). The TGA analysis of complexes 1-9 shows weight loss starting at 250, 280, 238, 115, 338, 198, 252, 378 and 294°C, respectively, depicting the stability of complexes.

DNA Binding studies

The DNA cleavage was controlled by the relaxation of supercoiled circular form of pBR322 DNA into the nicked and linear form. When a circular plasmid DNA is subjected to agarose gel electrophoresis, the fastest migration will be observed for supercoiled form (Form I). If one strand is cleaved, the supercoils will relax to produce a slower moving

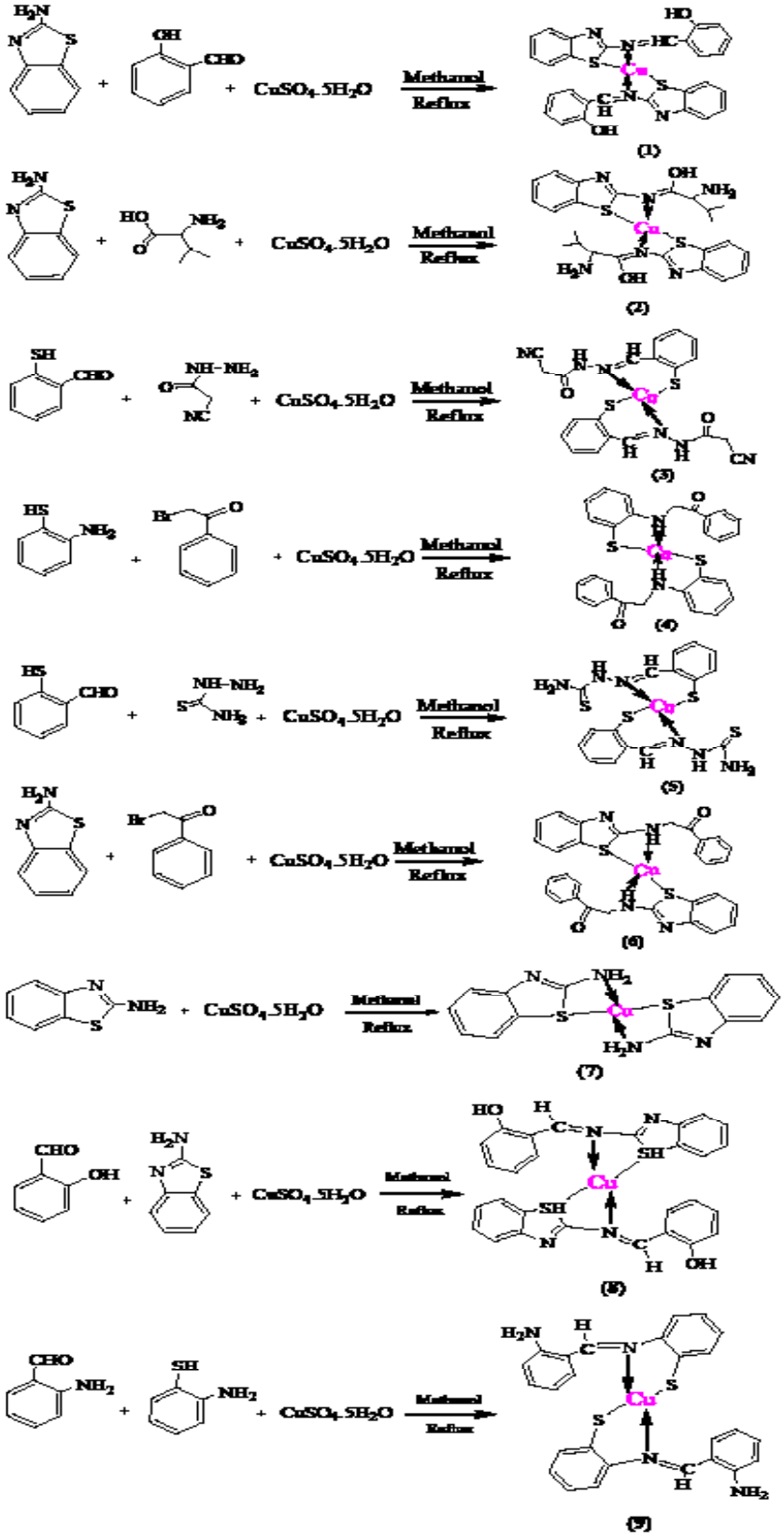

Scheme 1: Formation of Bis [2-(benzothiazol-2-yliminomethyl)-phenol] copper 1 and Bis [2-(benzothiazol-2-yliminomethyl)-valine] copper 2, Bis [cyanoaceto (2-mercaptobenzylidene)-hydrazide] copper 3, Bis [2-(phenacyl bromide)-aminothiophenol] copper 4, Bis [(2-mercaptobenzaldehyde) thiosemicarbazone] copper 5, Bis [N-(phenacyl bromide)-2-yliminobenzothiazole] copper 6, Bis (2-aminobenzothiazole) copper 7, Bis [2-(benzothiazol-2-yliminomethyl)-phenol] copper 8 and Bis 2-[(2'-aminobenzylidene)-amino]-benzenethiol copper 9.

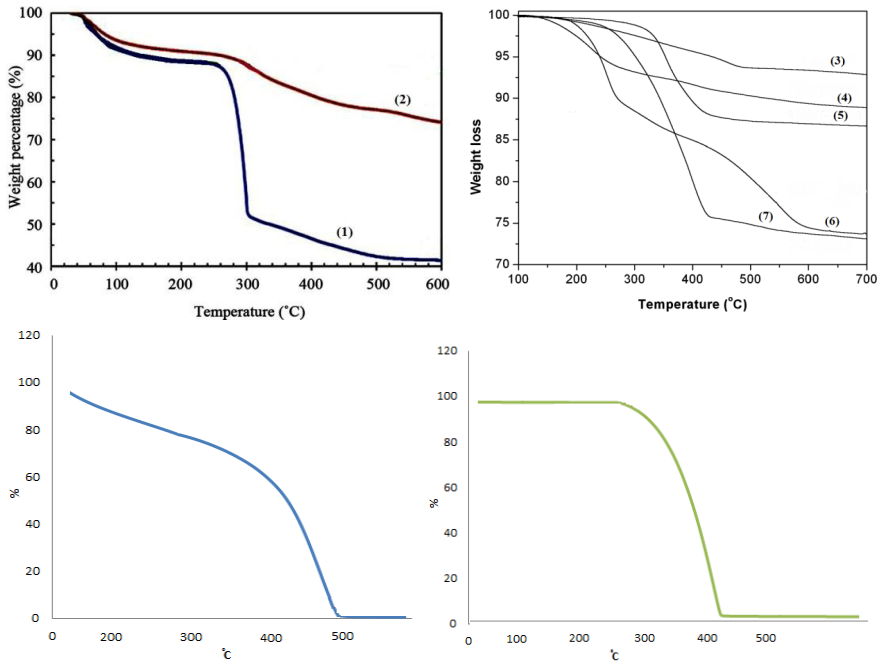

Figure 1: Thermo gravimetric analysis showing the thermal stability of complexes 1-9.

open circular form (Form II). If both strands are cleaved, a linear form (Form III) will be generated that migrates in between Form I and Form II. The DNA cleaving ability of complex 8 and 9 was investigated using pBR322 DNA. In the absence of any external additives the complex 8 and 9 cleaved double stranded supercoiled plasmid DNA (SC form: Form I) (300 ng) in 5 mM Tris–HCl / 50 mM NaCl buffer into nicked circular form (NC form: Form II) after 1 h of incubation at physiological pH 7.2 and temperature 25°C [24]. Keeping the DNA concentration constant (300 ng) the concentration of complex 8 and 9 was varied (1.0-7.0 μM) and the cleavage reaction was further monitored by gel electrophoresis. The results revealed concentration-dependent electrophoretic cleavage clearly showing the conversion of SC form (Form I) to NC form (Form II) with increase in concentration of complex 8 and 9.

At 3 μM concentration, complex 8 and 9 exhibited efficient nuclease activity. At still higher concentrations there was complete conversion of SC form into NC form with the concurrent formation of LC form. Presence of Form I, II, and III of pBR322 DNA indicated that complex 8 and 9 are involved in double strand DNA cleavage (Figures 2 and 3).

It is a well-known fact that DNA is the primary pharmacological target of number of anticancer drugs, and hence, the interaction between DNA and metal complexes are of paramount importance in understanding the mechanism. The interaction of transition metal complexes with DNA takes place via both covalent and / or non-covalent interactions. In the case of covalent binding, the labile ligand of the complexes is replaced by a nitrogen base of DNA such as guanine N7 while the non-covalent DNA interactions include intercalative, electrostatic and groove binding of metal complexes outside of a DNA helix [25]. The interaction of complexes 8 and 9 with CT DNA was examined by titrating the fixed amount of complexes with increasing concentration of CT DNA (5.3-2.6 × 10^{-5} M) as shown in Figure 4. The absorption spectra of complexes 8 and 9 indicated a blue shift in the wavelength on interaction with CT DNA as shown in Figure 4. This shift may be attributed to the change in environment around the metal centre [Cu(II)] as it may exhibit a preferential selectivity towards phosphate backbone. The spectral changes are typical of modes of interactions of DNA to substrate(s) that include hyperchromicity (blue shift) and hypochromicity (red shift). Hypochromic effect is attributed to the intercalative binding mode whereas hyperchromic effect might be ascribed to the electrostatic binding mode. The present data suggest a hyperchromism, which usually involve electrostatic interactions. It is also found that the binding of these complexes occur via the classical intercalation between the planar aromatic chromophores and DNA base pairs nevertheless the hyperchromic effect observed arises mainly due to the presence of Cu(II) ion which bind to DNA via electrostatic attraction to the phosphate group of DNA backbone and thereby causing a contraction and overall damage to the secondary structure of DNA.

To compare quantatively the effect of binding strength, the intrinsic binding constants (Kb) of the complexes 1 and 2 were determined by using Wolfe-Shimer equation [26] (Equation 1)

$$[DNA] / \varepsilon_a - \varepsilon_f = [DNA] / \varepsilon_b - \varepsilon_f + 1 / K_b \left| \varepsilon_b - \varepsilon_f \right| \quad (1)$$

where [DNA] represents the concentration of DNA, and ε_a, ε_f and ε_b the apparent extinction coefficient (A_{obs} / [M]), the extinction coefficient for free metal complex (M), and the extinction coefficient for the free metal complex (M) in the fully bound form, respectively. The K_b values for complexes 8 and 9 are 2.35 × 10^3 M^{-1} and 2.12 × 10^3 M^{-1}, respectively, which suggest that complex 8 has strong binding affinity for CT DNA as compared to complex 9.

In fluorescence spectral studies at room temperature, the complexes 8 and 9 emit luminescence at 374 nm respectively in 0.01 tris-HCl / 50 mM NaCl buffer when excited at 260 nm. Fixed amount of complexes 8 and 9 were titrated with increasing amount of CT DNA, over a range of 5.3-2.6 × 10^{-5} M DNA concentration. The addition of DNA caused a gradual increase in fluorescence emission (Figure 5) intensity being consistent with the non-intercalative binding mode such as electrostatic binding mode (surface binding) and be protected by DNA

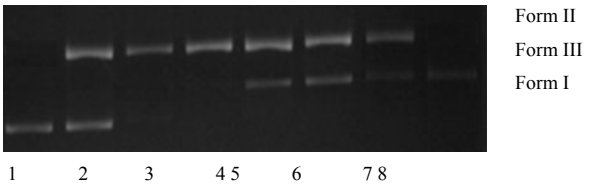

Figure 2: Agarose gel electrophoresis patterns of pBR322 plasmid DNA (300 ng) cleaved by complex 8 (1.0-7.0 μM), after 1 h incubation time (concentration dependent) Lane 1: control; Lane 2: 1.0 μM 1 + DNA; Lane 3: 2.0 μM 8 + DNA; Lane 4: 3.0 μM 8 + DNA. Lane 5: 4.0 μM 8 + DNA; Lane 6: 5.0 μM 8 + DNA, Lane 7: 6.0 μM 8 + DNA, Lane 8: 7.0 μM 8 + DNA in buffer (5 mM Tris-HCl/50 mM NaCl, pH 7.2 at 25°C).

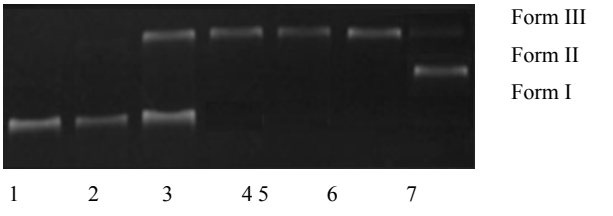

Figure 3: Agarose gel electrophoresis patterns of pBR322 plasmid DNA (300 ng) cleaved by complex 9 (1.0-6.0 μM), after 1 h incubation time (concentration dependent) Lane 1: control; Lane 2: 1.0 μM 9 + DNA; Lane 3: 2.0 μM 9 + DNA; Lane 4: 3.0 μM 9 + DNA. Lane 5: 4.0 μM 9 + DNA; Lane 6: 5.0 μM 9 + DNA, Lane 7: 6.0 μM 9 + DNA in buffer (5 mM Tris-HCl/50 mM NaCl, pH 7.2 at 25°C).

efficiently, since the hydrophobic environment inside the DNA helix reduces the accessibility of solvent molecule to the complex, which as a consequence restrict the complex mobility at binding site, leading to a decrease of the vibrational modes of relaxation and thus higher emission intensity [27]. Also, the number of bound copper complex per DNA (n) calculated [28] for complexes 8 and 9 were found to be 1.19 and 1.04, respectively from fluorescence spectral data.

The binding constant K, determined from the Scatchard equation for complexes 8 and 9 was calculated to be 1.83×10^3 and 1.45×10^3 M^{-1}, respectively which is in agreement with the similar trend of DNA binding ability (8 > 9) as observed in case of absorption spectral studies.

Treatment of supercoiled plasmid pBR322 DNA with complex 8 and detection of (˙OH) radicals

Cytotoxicity mechanism was confirmed by studying the treatment of supercoiled plasmid pBR322 DNA with different concentrations of complex 8 and 100 μM copper. Our nucleolytic experiments suggest that cell death may be due to cleavage or fragmentation of DNA of these cancer cells and that the active species responsible for this are ROS (˙OH) which resulted from the *in vitro* reaction of different concentrations of complex 8 with copper in presence of thiobarbituric acid. We observe from gel electrophoresis that after adding copper (100 μM) the concentration of radicals increase which in presence of different concentrations of complex 8 show the nicking of plasmid pBR322 DNA from its supercoiled form (Form I) to open circular form (Form II). As shown in lane 6, 7 and 8 (Figure 6), the nicking is quite obvious by the disappearance of form I and appearance of form II and with the increase in concentration of complex 8 (lane 8), the band intensity (form II) became maximum, depicting the more pronounced cleavage at high concentration.

In the DNA cleavage reactions mediated by various antioxidants in the presence of Cu (II), it has been established that Cu (II) is reduced to Cu (I) by the antioxidants and that Cu (I) is an essential intermediate in the DNA cleavage reactions. It is also generally understood that DNA cleavage by various antioxidants and Cu (II) is the result of the generation of hydroxyl radicals. Since Cu (II) is reduced to Cu (I) and the re-oxidation of Cu (I) to Cu (II) by molecular oxygen gives rise to superoxide anion which in turn leads to the formation of H_2O_2. Presumably Cu (I) is oxidized to Cu (II) by H_2O_2 in a Fenton type reaction giving rise to hydroxyl radicals. To determine the hydroxyl radical production and the role of copper ions in DNA cleavage, an experiment was performed where progressively increasing concentrations of complex 8 and Cisplatin (12.5-600 μM) were tested on thiobarbituric acid induced DNA breakage (Figure 7) and from these results we may conclude that the DNA cleavage by thiobarbituric acid involves endogenous copper ions (Cu (I) acts an intermediate) that leads to DNA cleavage.

The complex 8-Cu (II) (Figure 7A) and Cisplatin-Cu (II) (Figure 7B) are shown to generate the hydroxyl radicals (˙OH) which react with Calf thymus DNA, resulting in strand breaks. The assay is based on the fact that degredation of DNA by hydroxyl radical results in the release of TBA reactive material, which forms a coloured adduct readable at 532 nm. Increasing concentrations of complex 8 or Cisplatin in presence of Cu (II) showed a corresponding increase in the generation of hydroxyl radicals. The results in Figure 7 confirmed the relatively higher rate of formation of hydroxyl radicals and correlated with the rate of DNA degredation by the complex 8 as well as Cisplatin.

In vitro cytotoxicity

The anticancer activity *in vitro* was measured using the MTT assay during which the conversion of the soluble yellowish MTT to the insoluble purple formazan by active mitochondrial lactate dehydrogenase of living cells has been used to develop an assay system for measurement of cell proliferation [18,19]. The data reported in Table 1 suggests the During the cytotoxic screening of complexes 1-9, the potential behaviour was depicted against given cancer cells, during which the complex 1 showed IC_{50} = 4.29 μmol L^{-1} (SW–480), 4.91 μmol L^{-1} (HepG2), 5.64 μmol L^{-1} (HT-29) and 7.16 μmol L^{-1} (HL-60). Complex 2 also showed minimum IC_{50} value in the range of IC_{50} = 5.76 μmol L^{-1} (SW–480), 3.51 μmol L^{-1} (HepG2), 3.26 μmol L^{-1} (HT-29) and 6.61 μmol L^{-1} (HL-60) cell line. Complex 3 showed minimum IC_{50} value in the range of IC_{50} = 3.83 μmol L^{-1} (SW–480), 5.71 μmol L^{-1} (HepG2), 3.12 μmol L^{-1} (HT-29) and 4.18 μmol L^{-1} (HL-60) cell line. Complex 4 depicted minimum IC_{50} value in the range of IC_{50} = 4.82 μmol L^{-1} (SW–480), 5.28 μmol L^{-1} (HepG2), 3.31 μmol L^{-1} (HT-29) and 5.19 μmol L^{-1} (HL-60) cell line. Complex 5 depicted IC_{50} value in the range of IC_{50} = 4.88 μmol L^{-1} (SW–480), 4.64 μmol L^{-1} (HepG2), 4.87 μmol L^{-1} (HT-

IC_{50} (μM L^{-1})				
Complex	**SW480**	**HepG2**	**HT-29**	**HL-60**
1	4.29 ± 0.3	4.91 ± 0.4	5.64 ± 0.3	7.16 ± 0.4
2	5.76 ± 0.4	3.51 ± 0.4	3.26 ± 0.4	6.61 ± 0.4
3	3.83 ± 0.2	5.71 ± 0.1	3.12 ± 0.2	4.18 ± 0.3
4	4.82 ± 0.2	5.28 ± 0.4	3.31 ± 0.2	5.19 ± 0.2
5	4.88 ± 0.1	4.64 ± 0.2	4.87 ± 0.5	4.29 ± 0.2
6	6.47 ± 0.5	7.34 ± 0.6	5.92 ± 0.5	7.43 ± 0.6
7	3.77 ± 0.3	4.37 ± 0.1	5.23 ± 0.3	5.11 ± 0.4
8	5.31 ± 0.5	6.51 ± 0.6	5.91 ± 0.1	6.32 ± 0.5
9	4.63 ± 0.1	5.33 ± 0.3	4.29 ± 0.4	5.11 ± 0.1
Cisplatin	3.52 ± 0.1	5.91 ± 0.5	4.51 ± 0.3	7.37 ± 0.5

Table 1: The IC_{50} values of complexes 1-6 against given cancer cell lines.

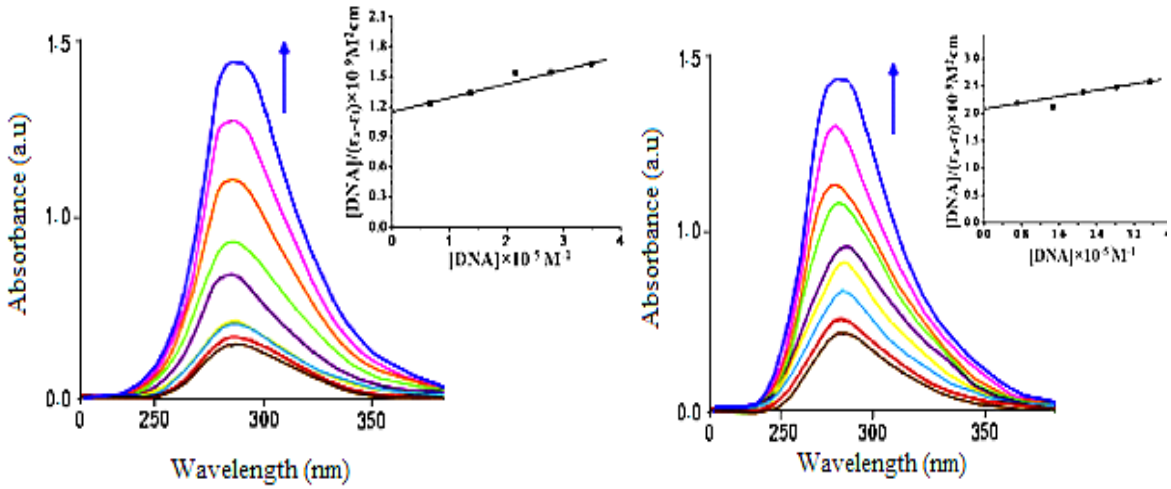

Figure 4: Absorption spectra of complexes 8 and 9 in Tris-HCl buffer upon the addition of calf thymus DNA [complex] = 6.67 × 10^{-6} M, [DNA] = 0.70 - 4.24 × 10^{-5} M. Arrow shows change in intensity with increasing concentration of DNA.

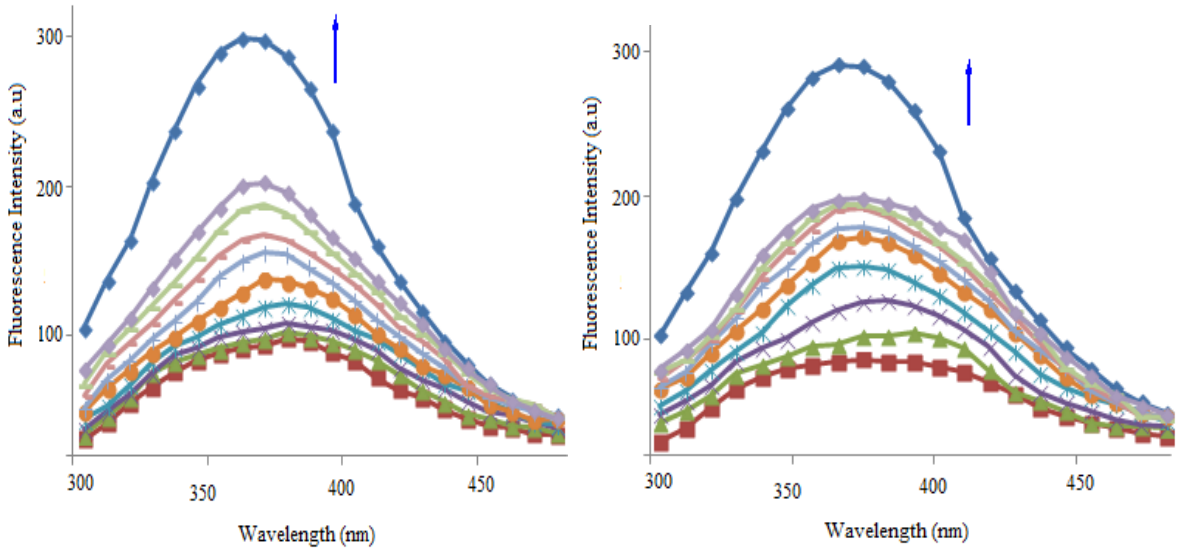

Figure 5: Emission spectra of compounds 8 and 9 in the presence of DNA in 5 mM Tris-HCl / 50 mM NaCl buffer. Arrows show the intensity changes upon increasing concentration of the DNA.

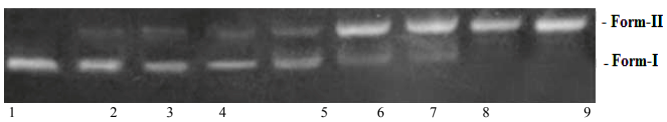

Figure 6: Fragmentation pattern of supercoiled plasmid pBR322, Lane 1 contains DNA only, lane 2 contains DNA and copper, lane 3, 4 and 5 contain DNA and complex 8 (100, 200 and 300 µM respectively), lane 6, 7 and 8 contain DNA and complex 8 (100, 200, 300 µM respectively) plus 100 µM copper and lane 9 contains DNA, Cisplatin (20 µM) plus 100 µM copper added to it.

29) and 4.29 µmol L^{-1} (HL-60) cell line. Complex 6 depicted IC_{50} value in the range of IC_{50} = 6.47 µmol L^{-1} (SW–480), 7.34 µmol L^{-1} (HepG2), 5.92 µmol L^{-1} (HT-29) and 7.43 µmol L^{-1} (HL-60) cell line. Complex 7 depicted IC_{50} value in the range of IC_{50} = 3.77 µmol L^{-1} (SW–480), 4.37 µmol L^{-1} (HepG2), 5.23 µmol L^{-1} (HT-29) and 5.11 µmol L^{-1} (HL-60) cell line. While as Complex 8 and 9 depicted IC_{50} value in the range of IC_{50} = 5.31, 4.63 µmol L^{-1} (SW–480), 6.51, 5.33 µmol L^{-1} (HepG2), 5.91, 4.29 µmol L^{-1} (HT-29) and 6.32, 5.11 µmol L^{-1} (HL-60) cell line. The screening data reveals that all the complexes showed promising anticancer activity by depicting inhibition count values close to the standard drug, Cisplatin. But complexes 2-5, 9 suppressed the cancer cell growth of HT-29 cells effectively than Cisplatin.

Microscopic examination of gross morphology of cancer cells and comparison with copper complex 8 treated normal and cancer cells is shown in Figure 8. The treatment of HT29 cells treated with the complex 8 10 µM (8A-8C) and complex 9 8 µM (8D-8F) is shown during which the decrease in the cell growth occur after 24 h but after 36 h treatment the cancer cells were almost dead.

Comet assay

In the comet assay, the images of HT-29 cells treated with complexes 8 and 9 showed the formation of comets. There was dose-dependent increase in tail length when treated with complexes 8 and

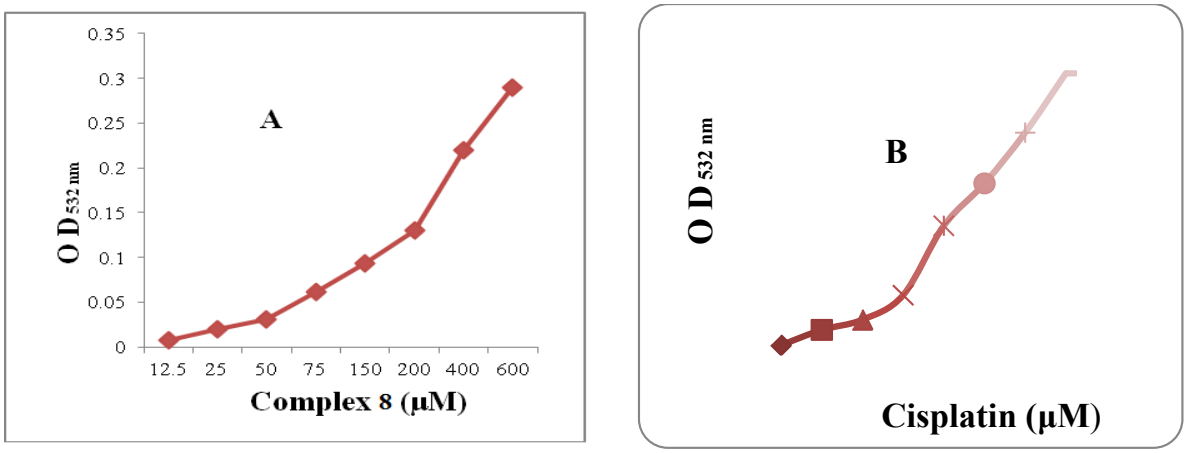

Figure 7: Comperative determination of hydroxyl radical production by complex 8 (A) and Cisplatin (B)by the assay of Thiobarbituric acid.

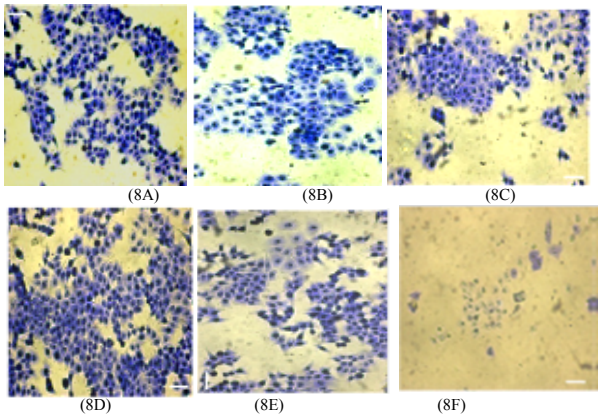

Figure 8: Confocal microscopy of HT29 cells treated with the complex 8 (8A-8C) and 9 (8D-8F) for 24 and 36 h.

9 (Figure 9). Complexes 8 and 9 showed genotoxic nature (formation of comet) which is in accordance with its maximum cytotoxicity as seen in MTT assay. The quantified increase in DNA damage suggested that the complexes 8 and 9 induced dose-dependent fragmentation of chromosomal DNA leading to apoptosis. The images of comet assay for positive control (cisplatin), cells treated with complexes 8 and 9 (10 µg/mL) are depicted in Figure 9. Slides were analysed for parameter like tail length (TL), using image analyzer CASP software version 1.2.2. The results of the tail length are shown in Figure 10.

Molecular docking studies with DNA

In our experiment, molecular docking studies of complex 8 and 9 with DNA duplex of sequence d(CGCGAATTCGCG)$_2$ dodecamer (PDB ID: 1BNA) were performed in order to predict the chosen binding site along with preferred orientation of the molecules inside the DNA groove. It is evident from the Figure 11 that the complex 8 recognizes the narrow minor groove region of DNA groove mainly through oxine ring and situated within slim A-T regions due to the planarity of the molecule because of two aromatic rings and preferential binding of oxine moiety to A-T regions leads to van der Waals and hydrophobic interaction with DNA functional groups which stabilizes the groove as well as the complex. The complex 9 showed the groove fit behaviour and arranged in a perpendicular manner with respect to the minor groove walls of the helix and stabilized by hydrogen bonding between the carbonyl group of oxine and NH of 6th Thiamine at a distance of 2.72 Å. The resulting binding energies of docked complexes 8 and 9 were found to be –278.1 KJ mol^{-1} and –284.94 KJ mol^{-1}, respectively which determine the stable binding as between DNA receptor and target ligand (Figure 11).

Physicochemical properties

Bioactivity score: The bioactivity scores of the complex 8 and 9 were also calculated for different parameters, GPCR (G protein-coupled receptor) ligand activity, ion channel modulation, kinase inhibition activity, protease inhibitor, enzyme inhibitor and nuclear receptor ligand activity. As we know for metal heterocyclic complexes, if the bioactivity score is more than 0.00 then the complex is active, but if it is between -0.50 and 0.00 then the complex is moderately active and if the complex has -0.50 then it is inactive. The potential bioactivity score of the complexes 8 and 9 is given in Table 2 which clearly shows that complexes show those properties which are required for the characteristics of complex for acting as a drug.

PASS analysis: Molecular properties such as membrane permeability and bioavailability are always associated with some basic molecular descriptors such as log P (partition coefficient), molecular weight (MW), hydrogen bond acceptors and donors count in a complex. Lipinski used these molecular properties in formulating his "Rule of Five". This rule states that most metal complexes with good membrane permeability have log P ≤ 5, number of hydrogen bond acceptors ≤ 10 and number of hydrogen bond donors ≤ 5. This rule is widely used as a filter for drug-like properties. The required complexes 8 and 9 showed good permeability by showing log P < 5 also the other parameters like topological surface area, molecular weight, hydrogen bond acceptor and hydrogen bond donor depicted that both complexes has potential to act as drug (Table 3). Also by considering the bioactivity score, the overall potential of the complexes can be said to be physiologically active.

Conclusion

In summary the development and operationally simple strategy for the better synthesis of copper complexes was successful. The reactions completed in almost 1-2 h and on completion, promising yields (75-82%) were obtained. From *in vitro* cytotoxicity screening, it is clear that copper complexes were found to be potential cytotoxic agents in comparison with standard drugs Cisplatin. Absorption and

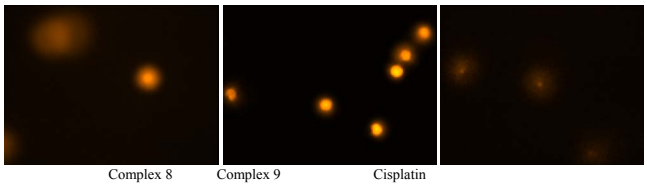

Figure 9: Detection of DNA damage in HT-29 cells. Treated cells (24 h) were layered over agarose gel, lysed, electrophoresed in alkaline buffer and stained with propidium iodide. The DNA fragmentation resulting in a comet-like appearance in cells treated with Cisplatin and complex 8 and 9.

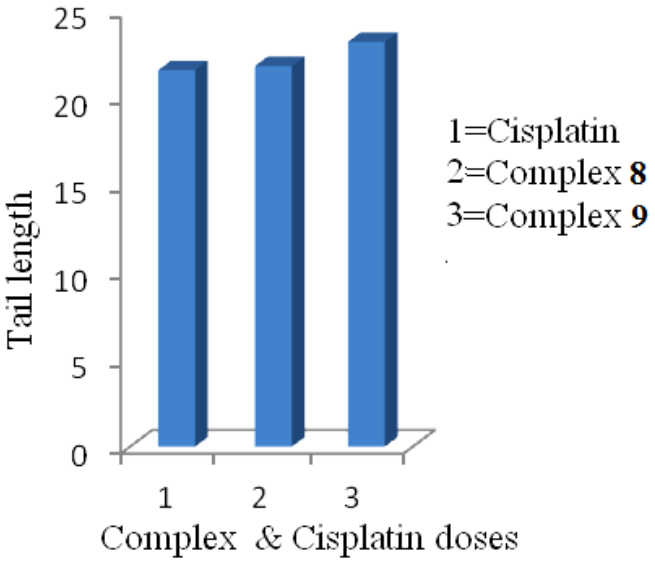

Figure 10: Diagram comparing the effect of copper complex 8 and 9 on the tail length in comet assay. Complex 8 and 9 caused maximum DNA damage among the two complexes in the comet assay. The extent of damage caused by copper complex 9 was more than the Cisplatin.

Parameters of Bioactivity score	Complex 8	Complex 9
G protein-coupled receptor ligand	0.83	0.97
Ion channel modulator	0.45	0.64
Kinase inhibitor	0.44	0.31
Nuclear receptor ligand	0.32	0.41
Protease inhibitor	0.53	0.47
Enzyme inhibitor	0.28	0.25

Table 2: Bioactivity score of the synthesized metal complex 8 and 9.

S.No	Lipinski rule of 5 parameters	Complex 8	complex 9
1	mi Log P	4.2	3.7
2	TPSA	22.26	24.71
3	HBA	6	2
4	HBD	0	2
5	N0-of rotatable bonds	2	2

1. The log P value calculated using mol inspiration server
2. Topological polar surface area (defined as a sum of surfaces of polar atoms in a molecule)
3. Hydrogen bond acceptor (expressed as the sum of O and N atoms)
4. Hydrogen bond donor (expressed as the sum of OH and NH)

Table 3: Physicochemical properties of the synthesized complex 8 and 9.

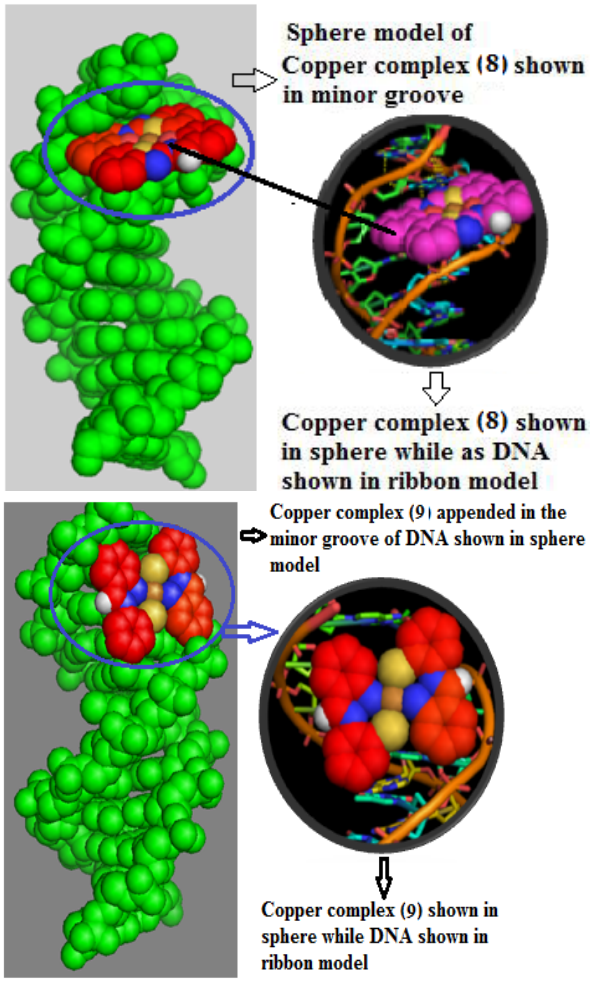

Figure 11: Docking models of DNA with complex 8 and 9 respectively, The N- and O termini of the [2-(Benzothiazol-2-yliminomethyl)-phenol and 2-[(2'-Aminobenzylidene)-amino]-benzenethiol of the complexes are shown as blue and red sticks, respectively.

fluorescence studies reveal the stabilization of the energy levels of the complexes in presence of DNA. The cleavage and molecular docking studies undertaken in the present work are in total agreement with the primary intercalative mode of binding, although the van der Waals and other types of interactions can also be argued. Bioactivity score and PASS analysis also depicted the drug nature of these complexes. Hence, the present study has shown that these synthesized complexes can be used as template for future development through modification and derivatization to design more potent and selective cytotoxic agents.

Acknowledgement

Authors thank the Chairman, Department of Chemistry, A.M.U., Aligarh, for providing necessary research facilities, the UGC for a research fellowship and SAP (DRS-I) for research support are also gratefully acknowledged. Authors thank Department of Biochemistry JNMC Aligarh for biological studies.

References

1. Mishra L, Yadav AK (2000) Exploring new-bioactive Ru(II) polypyridyl complexes through their interaction with DNA. Indian J Chem 39A: 660-663.
2. Pedrares AS, Romero J, Vazquez JAG, Duran ML, Casanova I, et al. (2003) Electrochemical synthesis and structural characterisation of zinc, cadmium and mercury complexes of heterocyclic bidentate ligands (N, S). Dalton Trans 7: 1379-1388.

3. Ekegren JK, Roth P, Kallstrom K, Tarnai T, Andersson PG (2003) Synthesis and evaluation of N,S-compounds as chiral ligands for transfer hydrogenation of acetophenone. Org Biomol Chem 1: 358-366.

4. Mevellec F, Tisato F, Refosco F, Roucoux A, Noiret N, et al. (2002) Synthesis and Characterization of the "Sulfur- Rich"Bis(perthiobenzoato) (dithiobenzoato) technetium (III) Heterocomplex. Inorg Chem 41: 598–601.

5. Kostova I (2006) Platinum complexes as anticancer agents. Recent Pat Anticancer Drug Discov 1: 1-22.

6. Guo Z, Sadler PJ (1999) Metals in Medicine. Angew Chem Int Ed 38: 1512-1531

7. Rosenberg B, Vancamp L, Krigas T (1965) Inhibition of Cell Division in *Escherichia coli* by Electrolysis Products from a Platinum Electrode. Nature 205: 698-699.

8. Tapiero H, Tew KD (2003) Trace elements in human physiology and pathology: zinc and metallothioneins. Biomed Pharmacother 57: 399-411.

9. Sarkar S, Mukherjee T, Sen S, Zangrando E, Chattopadhyay P (2010) Copper(II) complex of in situ formed 5-(2-pyridyl)-1,3,4-triazole through C–S bond cleavage in 1,2-bis(2-pyridyl methylthio)-bis-ethylsulphide: Synthesis, structural characterization and DNA binding study. J Mol Str 980: 117-123.

10. Marzano C, Pellei M, Tisato F, Santini C (2009) Copper complexes as anticancer agents. Anticancer Agents Med Chem 9: 185-211.

11. Turnlund JR, Keyes WR, Anderson HL, Acord LL (1989) Copper absorption and retention in young men at three levels of dietary copper by use of the stable isotope 65Cu. Am J Clin Nutr 49: 870-878.

12. De Vizcaya-Ruiz A, Rivero-Muller A, Ruiz-Ramirez L, Kass GE, Kelland LR, et al. (2000) Induction of apoptosis by a novel copper-based anticancer compound, casiopeina II, in L1210 murine leukaemia and CH1 human ovarian carcinoma cells. Toxicol *In Vitro* 14: 1-5.

13. Wallace DC (1999) Mitochondrial diseases in man and mouse. Science 283: 1482-1488.

14. Routier S, Bernier JL, Waring MJ, Colson P, Houssier C, Bailly C (1996) Synthesis of a functionalized salen-copper complex and its interaction with DNA. J Org Chem 61: 2326-2331.

15. Reicmann ME, Rice SA, Thomas CA, Doty P (1954) A Further Examination of the Molecular Weight and Size of Deoxypentose Nucleic Acid. J Am Chem Soc 76: 3047-3053.

16. Wolfe A, Shimer GH Jr, Meehan T (1987) Polycyclic aromatic hydrocarbons physically intercalate into duplex regions of denatured DNA. Biochemistry 26: 6392-6396.

17. Lakowicz JR, Weber G (1973) Quenching of fluorescence by oxygen. A probe for structural fluctuations in macromolecules. Biochemistry 12: 4161-4170.

18. Slater TF, Sawyer B, Straeuli U (1963) Studies on Succinate-Tetrazolium Reductase Systems. III. Points of Coupling of Four Different Tetrazolium Salts. Biochim Biophys Acta 77: 383-393.

19. Mosmann T (1983) Rapid colorimetric assay for cellular growth and survival: application to proliferation and cytotoxicity assays. J Immunol Methods 65: 55-63.

20. Woerdenbag HJ, Moskal TA, Pras N, MalingrÃ© TM, el-Feraly FS, et al. (1993) Cytotoxicity of artemisinin-related endoperoxides to Ehrlich ascites tumor cells. J Nat Prod 56: 849-856.

21. Singh NP (2000) Microgels for estimation of DNA strand breaks, DNA protein crosslinks and apoptosis. Mutat Res 455: 111-127.

22. Mustard D, Ritchie DW (2005) Docking essential dynamics eigen structures. Proteins 60: 269-274.

23. Delano WL (2002) The PyMOL Molecular Graphics System, DeLano Scientific, San Carlos.

24. Rajendiran V, Murali M, Suresh E, Palaniandavar M, Periasamy VS, et al. (2008) Non-covalent DNA binding and cytotoxicity of certain mixed-ligand ruthenium(II) complexes of 2,2'-dipyridylamine and diimines. Dalton Trans: 2157-2170.

25. Zhang QL, Liu JG, Chao H, Xue GQ, Ji LN (2001) DNA-binding and photocleavage studies of cobalt(III) polypyridyl complexes. J Inorg Biochem 83: 49-55.

26. Li Q, Yang P, Wang H, Guo M (1996) Diorganotin(IV) antitumor agent. (C2H5)2SnCl2 (phen)/nucleotides aqueous and solid-state coordination chemistry and its DNA binding studies. J Inorg Biochem 64: 181-195.

27. Chan HL, Ma DL, Yang M, Che CM (2003) Bis-intercalative dinuclear platinum(II) 6-phenyl-2,2'-bipyridine complexes exhibit enhanced DNA affinity but similar cytotoxicity compared to the mononuclear unit. J Biol Inorg Chem 8: 761-769.

28. Bourassa P, Kanakis CD, Tarantilis P, Pollissiou MG, Tajmir-Riahi HA (2010) Resveratrol, genistein, and curcumin bind bovine serum albumin. J Phys Chem B 114: 3348-3354.